Shaping Epigenetic Memory via Genomic Bookmarking

Davide Michieletto[1,†,*,‡], Michael Chiang[1,*], Davide Coli[2,*], Argyris Papantonis[3], Enzo Orlandini[2], Peter R. Cook[4], and Davide Marenduzzo[1,†]

[1] *School of Physics and Astronomy, University of Edinburgh, Peter Guthrie Tait Road, Edinburgh, EH9 3FD, UK.*

[2] *Dipartimento di Fisica e Astronomia and Sezione INFN, Universitá di Padova, Via Marzolo 8, Padova 35131, Italy*

[3] *Centre for Molecular Medicine, University of Cologne, Robert-Koch-Str. 21, D-50931, Cologne, DE*

[4] *The Sir William Dunn School of Pathology, South Parks Road, Oxford OX1 3RE, UK.*

∗ *Equal contribution*

† *corresponding author*

Reconciling the stability of epigenetic landscapes with the rapid turnover of histone modifications and their adaptability to external stimuli is an outstanding challenge. Here, we propose a new biophysical mechanism that can establish and maintain robust yet plastic epigenetic domains via genomic bookmarking (GBM). We model chromatin as a polymer whose segments bear non-permanent histone marks (or "colours") which can be modified by "writer" proteins. The three-dimensional chromatin organisation is mediated by protein bridges, or "readers", such as Polycomb-Repressive-Complexes and Transcription-Factors. The coupling between readers and writers drives spreading of biochemical marks and sustains the memory of local chromatin states across replication and mitosis. On the contrary, GBM-targeted perturbations destabilise the epigenetic landscape. Strikingly, we show that GBM can explain the full distribution of Polycomb marks in a whole Drosophila chromosome. Our model provides a starting point for an understanding of the biophysics of cellular differentiation and reprogramming.

INTRODUCTION

Cells belonging to distinct tissues in a multi-cellular organism possess exactly the same genome, yet the DNA sequence is expressed differently. This is made possible by the establishment of lineage-specific epigenetic landscapes – the heritable pattern of post-translational modifications (PTM) on histones and of methylation on DNA [1–8]. Epigenetic landscapes are robust, as they can be "remembered" across many rounds of cell division [1, 2, 7, 9–11]. At the same time, they are plastic and dynamic. They can adapt in response to external stimuli [1, 9, 12–14], and they are affected by disease and ageing [15–17]. Additionally, many biochemical marks encoding the epigenetic information can turn over rapidly and are lost during DNA replication [18, 19]. For example, acetyl groups on histones have half-lives < 10 minutes [18, 20], methyl groups on histones change during the period of one cell cycle [18, 21, 22] and DNA methylation is modified during development [17]. The turnover may originate from histone replacement/displacement during transcription [7, 18, 23], replication [7, 19, 24] or from stochastic PTM deposition and removal [25–27].

Our goal is to develop a biophysical model that can reconcile the reproducible and robust formation of heritable yet plastic epigenetic landscapes across cell populations in the face of the rapid turnover of the underlying histone marks. In particular we will be interested in models which can yield "epigenetic domains", by which we mean 1D stretches of similarly-marked histones which tend to be co-localised and co-regulated [28–32].

Existing models describe changes of PTMs in one-dimension (1D) or through effective long-range contacts; they yield smooth transitions between stable states and weak (transient) bistability [25, 26, 30, 33–37]. In contrast, our model explicitly takes into account the realistic structure and dynamics of the chromatin fibre in 3D (Fig. **1**) – crucial elements for the spreading of histone marks *in vivo* [11, 38–43].[Note that within the context of our model histone marks, chromatin states and and post-translational histone modifications (PTM) will be used interchangeably.]

From the physical perspective, accounting for realistic 3D interactions (e.g., the formation of loops and trans-contacts driven by the binding of bi- and multi-valent transcription factors) triggers "epigenetic memory" [7, 8], i.e., stability of the epigenetic landscape against extensive perturbations such as DNA replication [7, 44]. Within this framework, the possible "epigenetic phases" of the system are either disordered – no macroscopic epigenetic domain is formed – or homogeneous – only one histone mark spreads over the whole chromosome [44] (see Fig. **2**). Thus, no existing biophysical model can currently predict the sponta-

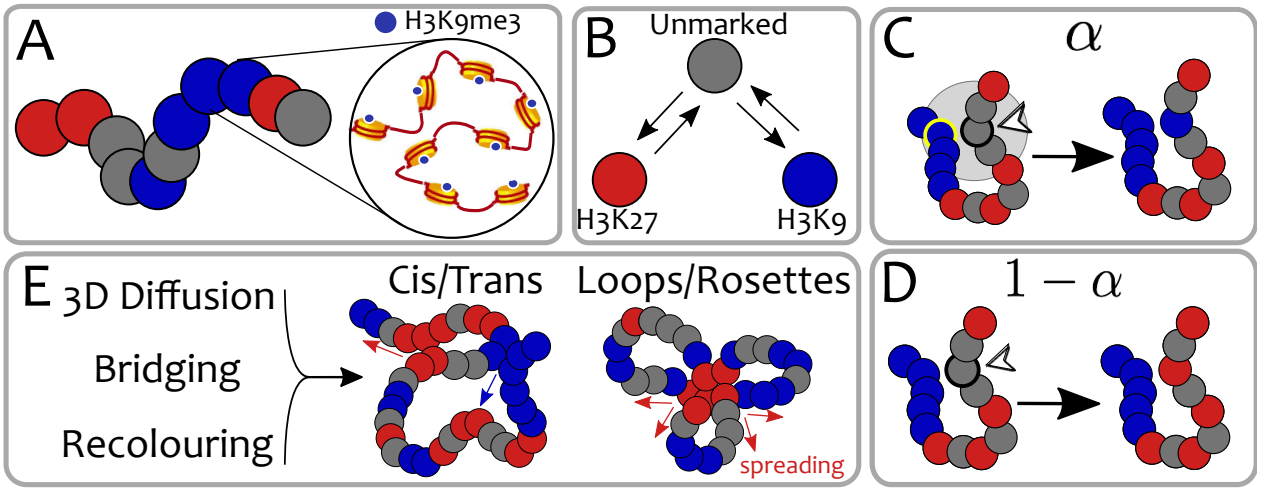

Figure 1. **A Polymer Model for Epigenetic Dynamics.** **(A)** In our coarse-grain polymer model, each bead represents a group of nucleosomes and its colour captures the predominant epigenetic mark. **(B)** Epigenetic marks are dynamic. They can change in between red, blue or grey (no mark) according to biophysical rules. For example, one can think of "red" as an inactive Polycomb state (marked by H3K27me3) or an active acetylated state (marked by H3K27ac) and "blue" as heterochromatic segments (with H3K9me3). The precise nature of the marks does not affect the qualitative behaviour of this generic model. In the Voter-like dynamics, each bead must go through the unmarked state (grey) before changing in the opposite colour [26]. Each bead is selected at rate k_R (see text and SM) and, **(C)** with probability α, it changes its colour "closer" to that of a randomly chosen 3D-proximal bead (in this case the one circled in yellow, see also SM). **(D)** The same bead has probability $1-\alpha$ to undergo a random colour conversion (in this case to red, see SM). **(E)** The synergy between 3D chromatin dynamics, bridging due to (implicit) binding-proteins/TFs and epigenetic recolouring gives rise to dynamical structures such as loop/rosettes and cis/trans contacts which drive (cis and trans) epigenetic spreading (indicated by red/blue arrows, see text).

neous emergence of multiple heritable epigenetic domains starting from a "blank" chromatin canvas [44].

Here, we propose a model for the *de novo* formation, spreading and inheritance of epigenetic domains that relies solely on three elements. First, we assume a positive feedback between multivalent PTM-binding proteins ("readers") and other proteins which depositing such marks ("writers"). This captures the well-known observations that, for instance, HP1 (a reader binding to heterochromatin) recruits SUV39h1 (a writer for H3K9me3 [45]), and that the Polycomb-Repressive-Complex PRC2 (a reader) contains the enhancer-of-zeste EZH2 (a writer) that spreads H3K27me3 [9, 18, 44, 46, 47]. Second, we assume the presence of genomic bookmarking (GBM) factors, typically transcription factors that can bind to their cognate sites and remain dynamically associated with chromatin through mitosis [48]. Examples of such GBMs include Polycomb-Group-Proteins (PcG) [11, 49–51], and Posterior-Sex-Combs (PSC) [52] bound to Polycomb-Response-Elements (PREs) in *Drosophila* [11, 39, 51, 52], GATA [53, 54] and UBF [55] in humans and Esrbb [56] and Sox2 [48, 57] in mouse. Here, we will use the term transcription factor (TF) to include both activators and repressors. Third, we assume that the recruitment of reading-writing machineries is coupled to specific GBM binding. These three assumptions allow our model to reconcile short-term turnover of PTM with long-term epigenetic memory and plasticity. Our model also quantitatively recapitulates the distribution of H3K27me3 mark seen in Drosophila *in vivo*.

RESULTS

A Polymer Model for Dynamical Epigenetic Landscapes

To capture the dynamic nature of the epigenetic landscape due to PTM turnover, we enhance the (semi-flexible) bead-spring polymer model for chromatin [60–68] by adding a further degree of freedom to each bead. Specifically, each bead – corresponding to one or few nucleosomes (the specific level of coarse-graining does not affect our qualitative results) – bears a "colour" representing the instantaneous local chromatin state (e.g., H3K9me3, H3K27me3, H3K27ac, etc., see Fig. **1**(A)), that can dynamically change in time according to realistic biophysical rules [25, 26, 44]. This is in contrast with previous works [30, 63, 69, 70] that only accounted for static landscapes.

We first consider a toy model in which beads may be found in one of three possible states: grey (unmarked), red (e.g., Polycomb-rich or acetylated) and blue (e.g., heterochromatin-rich). [A more realistic model will be discussed later]. Beads bearing the same histone mark are mutually "sticky", indicating the presence of implicit

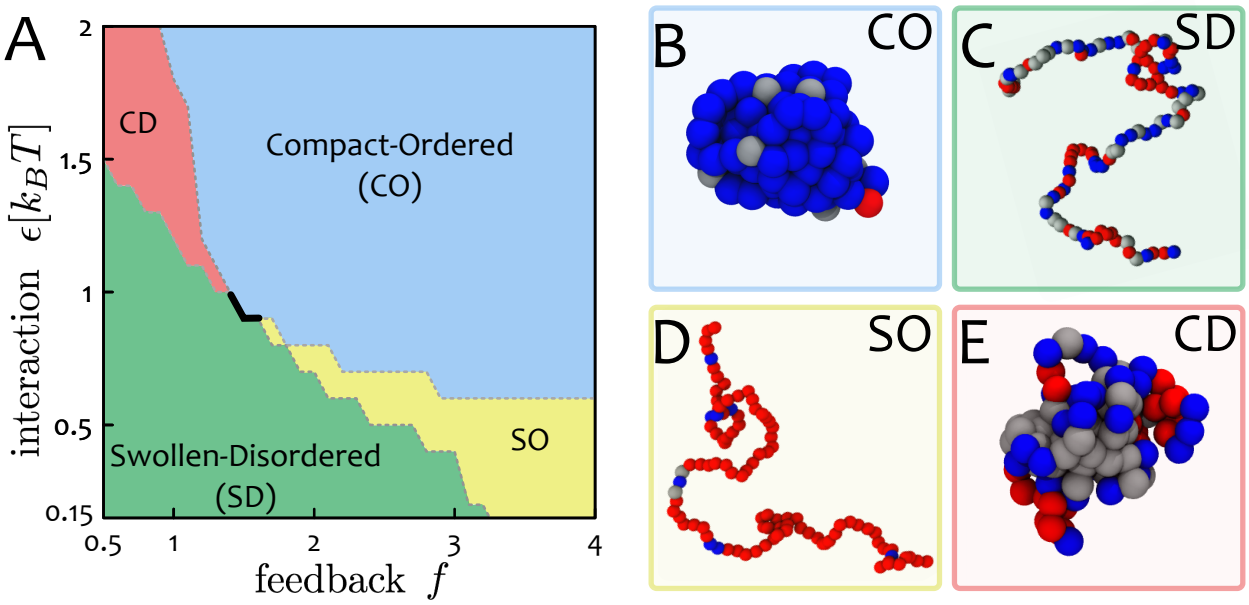

Figure 2. **Phase Diagram: Chromatin States and Epigenetic Memory.** **(A)** The phase diagram of the system in the space $(\epsilon, f \equiv \alpha/(1-\alpha))$ displays four distinct regions: (i) swollen-disordered (SD); (ii) compact-ordered (CO); (iii) swollen-ordered (SO) and (iv) compact-disordered (CD). The thick solid line represents a first-order transition between the SD and CO phases, whereas the dashed lines signal smoother transitions between the regions. (**B-E**) Representative snapshots of the stable states, which resemble conformations of chromatin seen *in vivo*. The CO phase may be associated to globally-repressed heterochromatin, the SO phase to open transcriptionally-active euchromatin while the CD phase to "gene deserts" characterised by low signal of PTMs and collapsed 3D conformations [28, 29, 58, 59]. The first-order nature of the SD-CO transition entails "epigenetic memory" [8], as the CO phase is robust against extensive perturbations such as the ones occurring during replication [44].

bridging proteins [18], and can thus bind to each other with interaction energy ϵ. All other interactions are purely repulsive. In addition, we model the action of writer proteins through "recolouring" moves occurring at rate k_R. We choose $k_R = 0.1s^{-1}$, close to typical timescales for acetylation marks [20]. In selected cases, we have also employed a faster recolouring rate of $k_R = 10s^{-1}$ to ensure faster convergence to steady state (see SM for details on simulations and time-mapping).

Our model couples reading and writing as follows. First, a bead is selected randomly. Next, with probability α, it recruits a neighbour from spatially-proximate beads (within $r_c = 2.5\sigma$, where σ is bead size). The colour of the first bead is then shifted one step "closer" to the colour of the second (Fig. **1**B-C). Otherwise (with probability 1-α), the bead undergoes a noisy conversion to one of the other colours (see Fig. **1**D and SM for further details).

This re-colouring scheme encodes a purely non-equilibrium process and it is akin to a "voter" or "infection-type" model [25, 26]. In SM, we describe a "Potts" recolouring scheme which can be arbitrarily tuned either in- or out-of-equilibrium [44]. Both schemes couple 1D epigenetic information along the chromatin strand to 3D folding. Both drive a positive feedback loop between readers (which bind and bridge chromatin segments) and writers (which can change the underlying epigenetic landscape [18]). Strikingly, both strategies lead to qualitatively similar behaviours, in which cis/trans contacts, globules and rosettes (Fig. **1**E) spontaneously emerge and drive the spread of histone modifications. To simplify the presentation of our results, and because the observed behaviours are similar, we choose to report in the main text the finding obtained via the "infection-type" model. This model may better capture the one-to-one nature of the chemical reactions required for the deposition (or writing) of histone marks (see SM for more details).

The Phase Diagram of the System Entails Epigenetic Memory

We first map the phase diagram obtained by varying the "feedback" parameter $f = \alpha/(1-\alpha)$ and the attraction energy ϵ/k_BT between any two like-coloured beads. A more realistic model accounting for different attractions between "Polycomb-rich" and "heterochromatin-rich" beads is considered later.

Figure **2**A shows that there are four distinct phases predicted by our minimal model. First, at small α and ϵ/k_BT the fibre is swollen and epigenetically disordered (SD). At large α and ϵ/k_BT, the system is in the compact epigenetically ordered (CO) phase. These two states are separated by a discontinuous transition, signalled by the presence of hysteresis and coexistence (see SM). The discontinuous

nature of the transition is important because it confers metastability to the two phases with respect to perturbations. Thus, perturbing a compact heterochromatin-rich state by extensively erasing PTM marks (e.g. during replication) fails to drive the system out of that epigenetic state [44]; in other words, the global epigenetic state is remembered during genome-wide re-organisation events [9, 44].

The two remaining regions of the phase diagram (Fig. **2**A) are (i) an ordered-swollen phase (SO), observed at large α but small or moderate ϵ/k_BT and (ii) a compact-disordered phase (CD), found at small α and large ϵ/k_BT. Our simulations suggest that the transitions from, or to, these states are smooth - unlike that between the SD and CO phases.

Polymer Simulations of the Minimal Model Recapitulate Realistic Chromosome Conformations

Intriguingly, some of the phases in the phase diagram in Fig. **2** correspond to structures seen in eukaryotic chromosomes. Most notably, the compact-ordered phase provides a primitive model for the structure of the inactive copy of the X chromosome in female mammals; this is almost entirely transcriptionally silent, and this state is inherited through many cell divisions [2]. The compact-disordered phase is reminiscent of "gene deserts" (or black chromatin [28, 58]) which have a low concentration of epigenetic marks, and which tend to co-localise in 3D due to self-attraction (possibly mediated by the linker histone H1 [28]). Finally, the swollen ordered phase is reminiscent of open and transcriptionally-active chromatin [59, 71, 72].

In this simplified model, feedback between readers and writers leads to unlimited spreading of a single histone mark in both ordered phases (CO and SO, see Fig. **2**) [44, 73]. Although near-unlimited spreading of silencing marks is seen in telomere position effects in yeast [38] and position-effect variegation in *Drosophila* [74]), this minimal model cannot recapitulate the existence of multiple epigenetic domains – or a "heterogeneous" epigenetic landscape.

A Biophysical Model for Genomic Bookmarking

We now introduce genomic bookmarking (GBM) to account for the coexistence of heritable epigenetic domains, and active/inactive (A/B) compartments [31, 32]. A bookmark is here considered as a TF (activator or repressor) that binds to a cognate site and recruits appropriate readers or writers (see Fig. **3**A).

A mechanistic model of how bookmarks might guide the re-establishment of the previous epigenetic landscape after mitosis remains elusive [17, 48, 54, 75]. Here, we assume that GBMs are expressed in a tissue-specific manner and remain (dynamically) associated to chromatin during mitosis [48, 52]. Then, on re-entering into inter-phase, they can recruit appropriate read/write machineries and re-set the previous transcriptional programme.

In our polymer model, we account for bookmarks by postulating that some of the beads cannot change their chromatin state (Fig. **3**A). Thus, a red (blue) bookmark is a red (blue) bead which cannot change its colour, and otherwise behaves like other red (blue) beads. In Figure **3**A, a bookmark is indicated by an orange square that binds to DNA (rather than a PTM) and recruits read/write machineries (e.g., PRC2), which then spread a histone mark (e.g., H3K27me3) to the neighbours [2, 5, 18, 76]. In our simulations, spreading is driven by the local increase in the density of red-rich (or blue-rich) segments, caused by like-colour attractions as this will increase the probability that at the next re-colouring move a red (blue) mark will be selected, thereby spreading that mark to 3D proximal beads.

GBM Drives the Stable Coexistence of 1D Epigenetic Domains and Shapes the 3D Chromatin Structure

We now consider a chromatin fibre with a fraction ϕ of bookmarks, so the total number of bookmarks is $Q = \phi L$; we analyse how their spatial distribution affects the epigenetic landscape in steady state. We consider three possible GBM distributions, as follows. (i) *Clustered*: Q bookmarks are equally spaced along the fibre; the colour alternates after every n_c consecutive bookmarks ($n_c > 1$ defines the cluster size). (ii) *Mixed:* same as clustered, but now colours alternate every other bookmark ($n_c = 1$). (iii) *Random:* bookmarks are placed and colours are chosen randomly along the fibre (ϕ is kept constant).

Figures **3**B-D show the results for $\phi = 0.1$ and a chromatin fibre $L = 1000$ beads long (corresponding to 3 Mbp, or 1.5×10^4 nucleosomes, for a coarse graining of 3 kbp per bead); thus, we assume a fibre with approximately one bookmarked bead every 150 nucleosomes. Simulations are initialised with the chromatin fibre in the swollen disordered phase (non-bookmarked regions contain equal numbers of red, blue and grey beads).

The clustered distribution of bookmarks (Fig. **3**B) quickly reaches a stable epigenetic landscape in which blocks of alternating colours (domains) alternate. On the contrary, the mixed bookmark pattern hinders domain formation, and the fibre remains in the SD state (Fig. **3**C). Remarkably, the random distribution also yields domains in 1D (Fig. **3**D), even in the absence of any correlation between the location of bookmarks.

Importantly, the bookmarking pattern affects 3D structure. Thus, in Figure **3**C-D, both the random and mixed patterns yield swollen or partially-collapsed fibres, even though the parameters used normally drive the system to a collapsed phase. [Note that our parameter choice ac-

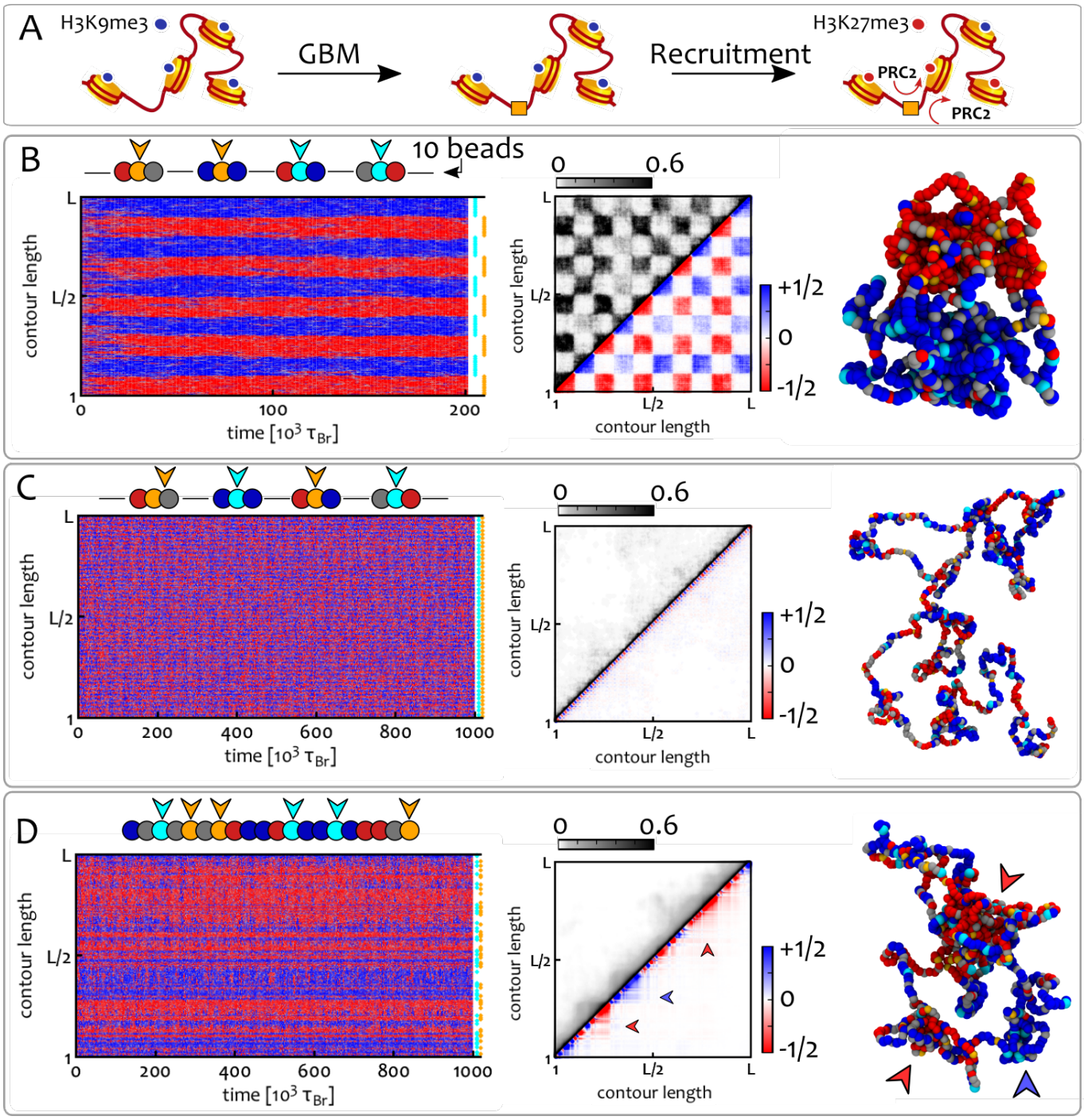

Figure 3. **GBM Shapes the Epigenetic Landscape and Chromatin Conformations.** (**A**) At the nucleosome level, GBM is mediated by a TF that binds to its cognate site and recruits read/write machineries that spread the respective histone mark to 3D-proximal histones (here PRC2 spreads H3K27me3). (**B-D**) We consider a chromatin fibre $L = 1000$ beads long, starting from an epigenetically random and swollen condition with $\phi = 0.1$, equivalent to one bookmark in 150 nucleosomes at 3kbp resolution and we fix $f = 2$ and $\epsilon/k_BT = 0.65$. GBM is modelled by imposing a permanent colour to some beads along the chromatin. Cyan and orange beads denote bookmarks for blue and red marks, respectively. Plots show kymographs (left column), average contact maps (central column) and typical snapshots (right column) for different bookmarking patterns (shown at the end of kymographs and cartoons above). Contact maps are split into two: the upper triangle shows a standard heat-map quantifying the normalised frequency of contacts between segments i and j, whereas the lower triangle shows an "epigenetically-weighted" one in which each contact is weighted by the type of beads involved (+1 for blue-blue contacts, -1 for red-red and 0 for mixed or grey-grey). (**B**) A clustered GBM pattern yields well-defined epigenetic domains which collapse into "A/B-like" compartments ($k_R = 0.1s^{-1}$). (**C**) Alternate GBM maintains the chromosome in a swollen-disordered state ($k_R = 10s^{-1}$). (**D**) Random GBM creates stable and coexisting TAD-like structures which are indicated by the arrowheads ($k_R = 10s^{-1}$).

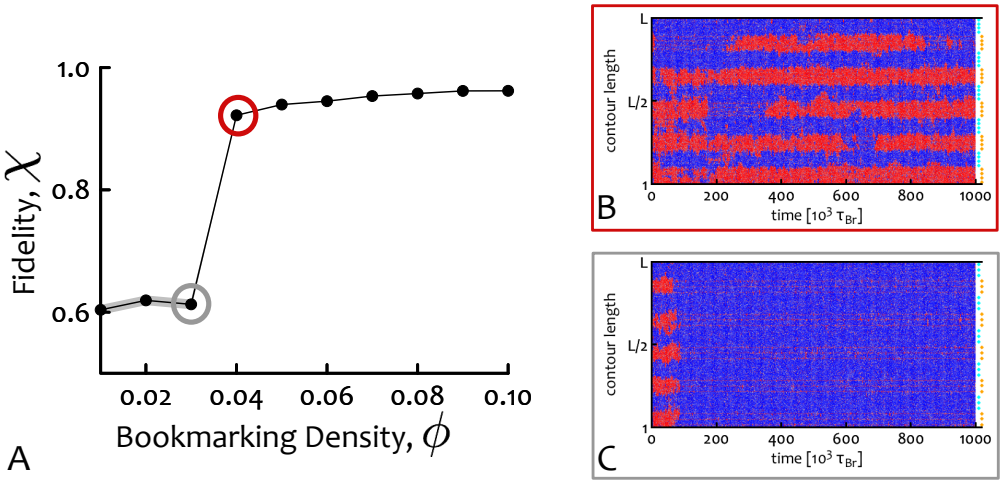

Figure 4. **A Critical Density of Bookmarks is Required for Stable Domain Formation.** (**A**) Using the clustered pattern of bookmarks at different densities ϕ we quantify the deviation from a "perfect" block-like epigenetic landscape. To do this we define the "fidelity", χ, as $1-\Delta^2$ where $\Delta^2 = Var\left[P_{\rm red}(i), \Pi(i)\right]$, i.e. the variance of the probability $P_{\rm red}(i)$ of observing a red bead at position i with respect to the perfect square wave $\Pi(i) = 0.5\left[{\rm sgn}\left(\sin\left(\pi i/n_d\right)\right)+1\right]$, where n_d is the number of beads in a domain (here $n_d = 100$). The fidelity χ jumps abruptly from a value near its lower bound of 1/2 towards unity, at the critical $\phi_c \simeq 0.04$. (**B,C**) Kymographs representing the behaviour of the system at the points circled in red and grey in (**A**).

counts for the fact that the critical $\epsilon(f)$ marking the SD-CO transition decreases with L.] For the random distribution, the contact map exhibits TAD-like structures, like those found in Hi-C data and long-range interactions between like-coloured domains are strongly suppressed (in contrast to equilibrium models with static epigenetic landscapes [30, 70]). On the other hand, for clustered bookmarks, red and blue domains separately coalesce in 3D (macro-phase-separation), to give a checker-board appearance of the contact map (Fig. **3**B) reminiscent of the patterns found in Hi-C data after suitable normalisation [77].

We suggest that the epigenetic landscape in eukaryotic cells may reflect a subtle combination of clustered and random bookmarking patterns to give local TAD-like structures embedded within a genome globally (micro-)phase-separated into A/B-compartments.

A Critical Density of Bookmarks is Required to Design Stable Domains

We now ask what is the minimum density of like-coloured bookmarks needed to form stable domains.

To address this question we systematically vary bookmark density and perform simulations with clustered patterns (Fig. **3**B) as these are the most effective to create domains. Here, ϕ varies from 0.01 to 0.1 for a chain with $L = 1000$ (i.e., $Q = 10-100$). To facilitate the analysis, we fix the domain size at 100 beads (300 kbp), which is in the range of typical HiC domains [31, 32, 77]. Then, there can be a maximum of 10 domains in the simulation (this is achieved by adjusting n_c as ϕ changes). To enhance domain formation, we use $\epsilon/k_BT = 1$, while keeping $f = 2$. To quantify the efficiency of domain formation, we measure the probability that bead i ($1 \le i \le L$) is in a "red" state, $P_{\rm red}(i)$. If ideal regular domains are formed along the fibre (i.e., if all beads have the intended colour, that of the closest bookmarks) then $P_{\rm red}(i)$ would be a perfect square wave $\Pi(i)$ (Fig. **4**, caption). The fidelity of domain formation can then be estimated as $\chi = 1-\Delta^2$, where Δ^2 is the mean square deviation (variance) between $P_{\rm red}(i)$, measured in simulations, and $\Pi(i)$, i.e. $\Delta^2 = \sum_{i=1}^{L}\left[P_{\rm red}(i)-\Pi(i)\right]^2/L$. The value of $\chi = 1-\Delta^2$ is low, and approaches 1/2, when the epigenetic landscape is far from the ordered block-like state, and is dominated by a single colour, whereas it tends to unity, for ideal block-like domain formation.

Figure **4**A shows the fidelity of domain formation, χ, as a function of bookmark density, ϕ. As expected from previous results, there is a phase transition at a critical density $\phi_c \simeq 0.04$. For $\phi > \phi_c$, stable domains are seen in kymographs and $\chi \simeq 1$ (see also previous Fig. **3**B). For $\phi < \phi_c$ a single mark takes over the fibre. Near $\phi = \phi_c = 0.04$ there is a sharp transition between these two regimes in which domains appear and disappear throughout the simulation (see kymograph in Fig. **4**B). This critical density may correspond to $1-10$ nucleosomes in about 400 as not all nucleosomes in a bookmark bead need to be bookmarked.

Crucially, not all the genome must have this critical density of bookmarks, but only regions required to robustly develop a specific domain of coherent PTM in a given cell-line.

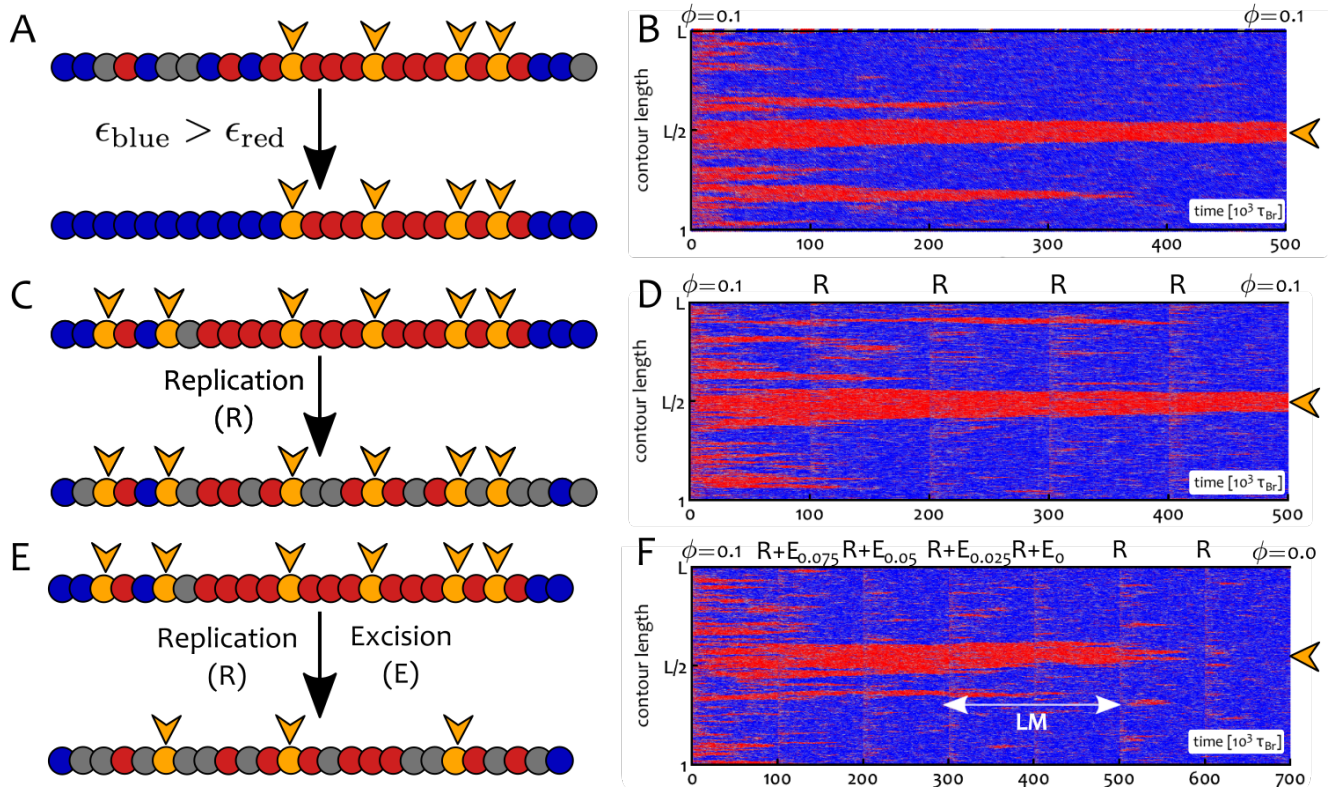

Figure 5. **Asymmetric Interactions and Bookmark Excision but not DNA Replication Affect the Epigenetic Landscape.** (**A-B**) Here we consider the case in which blue-blue interactions are stronger than red-red ones. Specifically, we set $\epsilon_{\text{blue}} = 1k_BT$ and $\epsilon_{\text{red}} = 0.65k_BT$ with $f = 2$. The central region of a chromatin segment $L = 2000$ beads long is initially patterned with bookmarks at density $\phi = 0.1 > \phi_c$ (the region in the kymograph is indicated by an orange arrowhead). Blue beads invade non-bookmarked regions thanks to the thermodynamic bias whereas the local red state is protected by the bookmarks. (**C-D**) The chromatin fibre undergoes replication cycles which extensively perturb the pattern of PTM of histones on chromatin. A semi-conservative replication event (R) occurs every 10^5 τ_{Br} and half of the (non-bookmarked) beads become grey. The epigenetic landscape is robustly inherited. (**E-F**) The chromatin fibre undergoes semi-conservative replication followed by excision of bookmarks (R+E). At each time, 1/4 of the initial bookmarks are removed and turned into grey (recolourable) beads. The epigenetic landscape is inherited until $\phi < \phi_c$. At this point, the central red domain is either immediately lost (not shown) or it can be sustained through some replication cycles (**F**) by local memory (LM).

Biasing Stability with Asymmetric Interactions

Thus far, we have considered symmetric interactions between like-coloured beads. In other words, red-red and blue-blue interaction strengths were equal. However, such binding energies may differ if mediated by distinct proteins. Consider the case where red and blue marks encode Polycomb repression and constitutive heterochromatin, respectively. If the blue-blue interaction is larger than the red-red one, the thermodynamic symmetry of the system is broken and the blue mark eventually takes over a non-bookmarked chromatin region (Fig. **5**A). However, if there are bookmarks for the red state, they locally favour the red state, whereas the stronger attraction globally favours the blue mark. This competition creates an additional route to stable domains as exemplified in Figure **5**A,B. Here, red bookmarks (identified by orange beads) are concentrated in the central segment of a chromatin fibre. Starting from a swollen and epigenetically disordered fibre, where red, blue and grey beads are equal in number, we observe that blue marks quickly invade non-bookmarked regions and convert red beads into blue ones (a process mimicking heterochromatic spreading *in vivo* [45]). However, the central segment containing the bookmarks displays a stable red domain (Fig. **5**A,B).

Bookmark Excision but not DNA Replication Destabilises the Epigenetic Landscape

We next asked whether the epigenetic landscape established through GBM is also stable against extensive perturbations such as DNA replication. In order to investigate this we simulated semi-conservative replication of the chromatin fibre by replacing half of the (non-bookmarked) beads with new randomly coloured beads. In Figure **5**C-D we show that, in agreement with the results of Figures **3**

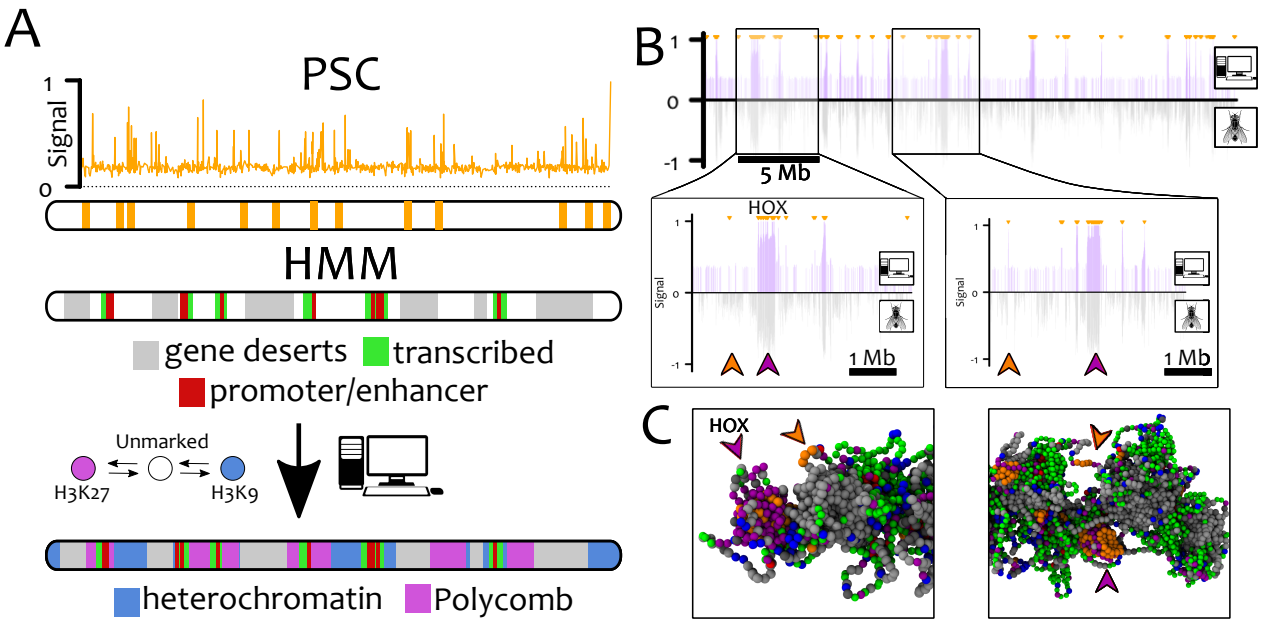

Figure 6. **GBM is Sufficient to Recapitulate the Distribution of Polycomb Marks in *Drosophila* S2 cells.** In this figure, we apply our GBM model to a realistic scenario: We perform chromosome-wide simulations of Ch3R of Drosophila S2 cells at 3 kbp resolution ($L = 9302$). (**A**) The location of PSC/PRE bookmarks are mapped onto beads using ChIP-Seq data [52]. Using results from the "9-states" HMM [58], gene deserts (regions lacking any mark in ChIP-seq data, state 9), promoter/enhancers (state 1) and transcriptionally active regions (states 2-4) are permanently coloured grey, red and green, respectively. The remaining beads are initially unmarked (white) and may become either heterochromatin (states 7,8 – blue) or polycomb (state 6 – purple). (**B**) *In silico* ChIP-seq data for H3K27me3 (top half, purple lines) is compared with *in vivo* ChIP-seq [58] (bottom half, grey line). Small orange arrow at the top of the profile indicate the location of the bookmarks. The excellent quantitative agreement between the datasets is captured by the Pearson correlation coefficient which is $\rho = 0.46$ – to be compared with $\rho = 0.006$ obtained between a random and the experimental datasets. We highlight that not all the bookmarked beads foster the nucleation of H3K27me3 domain (see big purple/orange arrowheads in the insets, corresponding to the HOX cluster). The reason can be found by analysing the 3D conformations of the chromosome (**C**). The non-nucleating bookmarks (orange arrowheads), although near in 1D, are found far from potential target beads in 3D space (purple arrowheads) and so fail to yield large H3K27me3 domains.

and **4**, our model can "remember" the established epigenetic landscape through multiple rounds of cell division. Importantly, the combination of "memory" [8] and local epigenetic order (via bookmarks) may allow cells to display epialleles with different transcriptional behaviours (local or "cis-" memory [27, 78]).

We next considered a set-up relevant in light of recent experiments in *Drosophila* [51, 79], where the role of PRE in epigenetic memory was investigated. In these works, polycomb-meditated gene repression was perturbed as a consequence of artificial insertion or deletion of Polycomb-Response-Elements (PREs). In Figure **5** we therefore performed a simulated dynamical experiment where replication was accompanied by random excision of bookmarks [51] (Fig. **5**E,F); in practice, we remove 1/4 of the initial number of bookmarks at each replication event. Then each "cell cycle" successively dilutes the bookmarks which at some point can no longer sustain the local red state and the region is consequently flooded with blue marks. Importantly, the system does not display the immediate loss of the red domain as soon as $\phi < \phi_c$; on the contrary, this domain is temporarily retained through local memory [9, 27, 78], which originates from enhanced local density of marks together with the positive read/write feedback (see SM). These results are again consistent with those found experimentally, where regions marked with H3K27me3 are only gradually lost after PRE excision [51].

Chromosome-Wide Simulations Recapitulate Epigenetic Landscapes in *Drosophila*

Simplified models considered thus far are useful to identify generic mechanisms; we now aim to test our model on a realistic scenario. To do so, we perform polymer simulations of the whole right arm of chromosome 3 in *Drosophila* S2 cells.

Bookmarks (orange, in Fig. **6**) are located on the chromosome using PSC ChIP-Seq data [52], as PSC binds to PREs during inter-phase and mitosis [52] as well as recruiting PRC2 (via molecular bridging). Some other beads are permanently coloured according to the "9-state" Hidden Markov Model (HMM, [58]). If they correspond to gene deserts (state 9), promoter/enhancers (state 1) or transcriptionally active regions (states 2-4) they are coloured

grey, red and green, respectively. We further introduce an interaction between promoter and enhancer beads to favour looping, plus, an attractive interaction between gene desert (grey) beads mimicking their compaction by H1 linker histone [28] (see SM for full list of parameters). The remaining 20% of the polymer is left blank and these "unmarked" beads are allowed to dynamically change their chromatin state into heterochromatin (blue) or polycomb (purple) according to our recolouring scheme.

We evolve the system to steady state and we evaluate the probability of finding a Polycomb mark at a certain genomic position [80]. This provides us with an *in silico* ChIP-seq track for polycomb marks which can be compared with *in vivo* ChIP-Seq data [58] (see Fig. **6**B). The two are in good agreement (Pearson correlation coefficient $\rho = 0.46$, against $\rho = 0.006$ for a random dataset).

Remarkably, not all bookmarked segments (orange) are populated by Polycomb marks; instead we observe that H3K27me3 spreading requires appropriate 3D folding (Fig. **6**B-C, insets). Bookmarks which do not contact other bookmarks due to the local epigenetic landscape do not nucleate H3K27me3 spreading. Again, this is consistent with 3D chromatin conformation being crucial for the spreading and establishment of epigenetic landscapes [11, 40, 43].

DISCUSSION

We proposed and investigated a new biophysical mechanism for the *de novo* establishment of epigenetic domains and their maintenance through interphase and mitosis. Our simplest model requires only one element: a positive feedback between readers (e.g., binding proteins HP1, PRC2, etc.) and writers (e.g., methyltransferases SUV39, EzH2, etc.).

We performed large-scale simulations in which chromatin is modelled as a semi-flexible bead-and-spring polymer chain [60–62, 66] overlaid with a further degree of freedom representing the dynamic epigenetic landscape [44, 73]. Specifically, each bead is assigned a colour corresponding to the local instantaneous epigenetic state (e.g., unmarked, polycomb- or acetylation-rich (red) and heterochromatin-rich (blue)). Readers are implicitly included by setting an attraction between like-coloured beads [63, 70], whereas writers are modelled by performing re-colouring moves according to realistic and out-of-equilibrium rules [26, 34] (see Fig. **1**). Intriguingly, we note that the main qualitative behaviours are retained when detailed balance is restored [44] (see SI).

If read-write positive feedback is sufficiently strong, a single histone mark can spread through an epigenetically "disordered" fibre to induce a discontinuous transition to a collapsed-ordered state (see Fig. **2**). The dominant histone mark is either the one corresponding to the strongest 3D attraction (Fig. **5**) or is selected by spontaneous symmetry-breaking if 3D attractions are equal (Fig. **2**). The compact-ordered structure is stable: even if some beads lose their colour, their neighbours can restore it quickly. This "epigenetic memory" renders our chromatin model robust against extensive perturbations, such as those occurring during replication [5, 18, 38], when most histones are removed or displaced [2, 18].

The main limitation of this simple model is that epigenetic order in real chromosomes is local, rather than global. Multiple epigenetic domains – each with one mark – coexist on a chromosome [32], thereby forming an "heterogeneous" epigenetic landscape. Our main result is that our model predicts the formation of heterogeneous epigenetic landscapes which can be inherited when we include genomic bookmarking (GBM).

Bookmarks are usually considered to be transcription factors that remain (dynamically) associated through mitosis so gene activity can be inherited from one interphase to the next [54, 57, 75]. We envisage bookmarks perform an additional function which is typical of many TFs: they recruit read/write machineries, and hence nucleate the spreading of epigenetic marks and the establishment of epigenetic domains. Here we assumed bookmarking TFs are permanently bound to DNA, however our conclusions should hold even for dynamic bookmarks that switch between bound and unbound state [48, 81].

Stable domains can be formed with only one type of bookmark, when the competing histone mark is thermodynamically favoured (Fig. **5**). This result rationalises the common understanding that heterochromatin can spread at lengths (blue mark in Fig. **5**A,B) and it is stopped by actively transcribed (bookmarked) regions. Further, it is in agreement with recent genome editing experiments in *Drosophila*: when PRE is inserted into the genome, it provides a bookmark for H3K27me3 which leads to spreading of that mark [51], whereas PRE excision leads to (gradual) loss of the mark [51]. These findings can be readily explained within our model if the 3D attraction between polycomb marks is slightly weaker than that between, e.g., H3K9me3-modified regions (Fig. **5**). Additionally, the expression of HOX and other Polycomb-regulated genes (which contain multiple PREs) is less sensitive to deletion of single PREs [82]. We suggest that this is because domains remain stable as long as bookmark density is kept above the critical threshold (Fig. **4**).

Our results thus strongly suggest that bookmarks are key elements that allow cells to access and maintain the correct "memory" of the previous epigenetic landscapes. Losing bookmarks (via artificial excision or DNA mutation) will thus impair the ability of cells to inherit the cell-line-specific epigenetic landscape. In addition, we argue that newly activated bookmarks (for instance subsequently to inflammation response or external stimuli [13, 14, 83]) may drive the *de novo* formation of transient epigenetic domains which allow the plastic epigenetic response to environmental changes.

Our model also recreates the pattern of H3K27me3 in

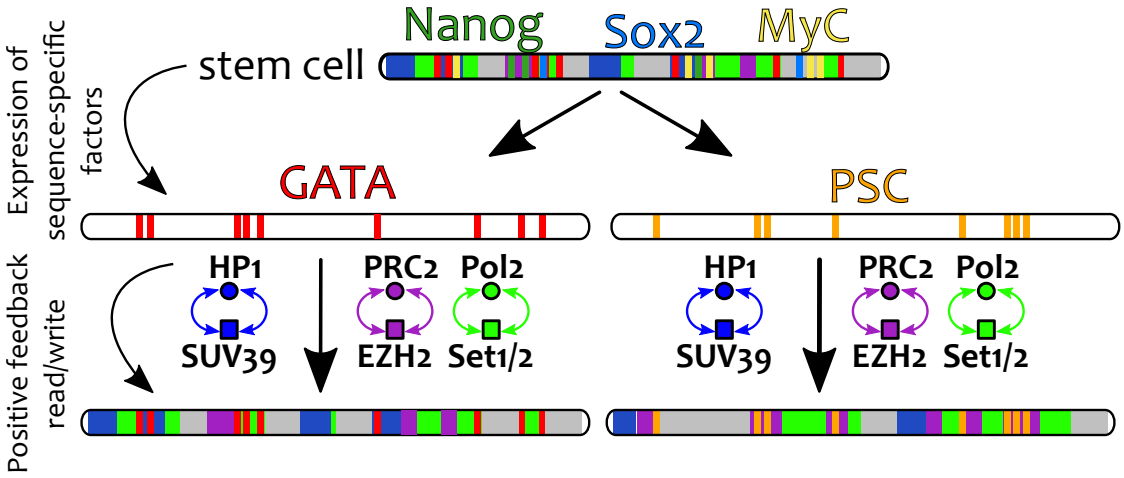

Figure 7. **Model for Cellular Differentiation**. We speculate that cellular differentiation may be driven by a two-step process. First, sequence-specific factors (bookmarks) are expressed as a consequence of environmental and positional cues. Second, the positive feedback set up by read/write machineries drives the establishment and maintenance of tissue-specific epigenetic landscapes. As a consequence, genomic bookmarks are key targets to understand cellular differentiation and reprogramming.

Drosophila S2 cells. Here, GBM by PSC leads to epigenetic spreading within a pattern of active TFs, and inactive gene deserts. Besides being quantitatively accurate, our simulations show that not all PRE bookmarks end up in H3K27me3 domains: whether or not they do, depends on their network of chromatin contacts in 3D, as highlighted experimentally in [11, 40, 43]. This is also reminiscent of the well-known position effect according to which the activity of a gene depends on its local environment [14].

Our results also prompt several further questions. First, starting from a stem cell, how might different cell lineages be established? We suggest that environmental and morphological cues trigger production of lineage-specific bookmarks such as GATA [54] and PSC [52], which trigger the positive feedback between readers and writers to generate and sustain new epigenetic landscapes (Fig. **7**). Thus, bookmarks are here envisaged as key elements that should be targeted in order to understand, and manipulate, cellular differentiation. Second, how might reprogramming factors like Sox2, Nanog, and Myc work? Possibly, their binding generates alternative feedback cycles that mask [15] the action of pre-existing bookmarks, thereby allowing other bookmarks to establish new epigenetic landscapes.

We have extended the existing notion of GBM [54, 57, 75, 84] to include the direct recruitment of read/write machineries. This coupling allows our model to predict the *de novo* establishment of heterogeneous epigenetic landscapes which can be remembered across replication and can adapt to GBM-targeted perturbations.

Within our framework, architectural elements such as CTCF [2], Cohesins [61] and SAF-A [72] may provide the initial 3D chromatin conformation upon which the GBM-driven establishment of epigenetic landscape takes place [11, 40, 43].

Author Contribution

D.Mi.,A.P.,E.O.,P.R.C. and D.Ma. designed research and discussed results. D.Mi.,M.C.,D.C. performed simulations. All authors wrote the paper.

Acknowledgements

We acknowledge the European Research Council for funding (Consolidator Grant THREEDCELLPHYSICS, Ref. 648050). Work in the Papantonis lab is supported by CMMC core funding. The authors thank C. A. Brackley, A. Buckle, N. Gilbert and J. Allan for insightful remarks on the manuscript.

[1] C. H. Waddington, Nature **150**, 563 (1942).
[2] B. Alberts, A. Johnson, J. Lewis, D. Morgan, and M. Raff, *Molecular Biology of the Cell* (Taylor & Francis, 2014) p. 1464.
[3] B. Strahl and C. Allis, Nature **403**, 41 (2000).
[4] T. Jenuwein and C. D. Allis, Science **293**, 1074 (2001).
[5] G. Cavalli and T. Misteli, Nat. Struct. Mol. Biol. **20**, 290 (2013).
[6] B. Pal, T. Bouras, W. Shi, F. Vaillant, J. M. Sheridan, N. Fu, K. Breslin, K. Jiang, M. E. Ritchie, M. Young, G. J. Lindeman, G. K. Smyth, and J. E. Visvader, Cell Rep. **3**, 411 (2013).
[7] A. V. Probst, E. Dunleavy, and G. Almouzni, Nat. Rev. Mol. Cell. Biol. **10**, 192 (2009).
[8] R. K. Ng and J. B. Gurdon, Nat. Cell Biol. **10**, 102 (2008).
[9] A. Angel, J. Song, C. Dean, and M. Howard, Nature **476**, 105 (2011).
[10] A. Kouskouti and I. Talianidis, EMBO J. **24**, 347 (2005).

[11] F. Ciabrelli, F. Comoglio, S. Fellous, B. Bonev, M. Ninova, Q. Szabo, A. Xuéreb, C. Klopp, A. Aravin, R. Paro, F. Bantignies, and G. Cavalli, Nat. Genet. (2017).

[12] S. Stern, Y. Fridmann-Sirkis, E. Braun, and Y. Soen, Cell Rep. **1**, 528 (2012).

[13] S. Wood and A. Loudon, J. Endocrinol. **222** (2014).

[14] A. Feuerborn and P. R. Cook, Trends Genet. **31**, 483 (2015).

[15] A. Zirkel, M. Nikolic, K. Sofiadis, J.-P. Mallm, L. Brant, C. Becker, J. Altmueller, J. Franzen, M. Koker, E. G. Gusmao, I. G. Costa, R. T. Ullrich, W. Wagner, P. Nuernberg, K. Rippe, and A. Papantonis, bioRxiv **144** (2017).

[16] S. Pal and J. Tyler, Sci. Adv. **2**, 253 (2016).

[17] E. Heard and R. A. Martienssen, Cell **157**, 95 (2014).

[18] G. E. Zentner and S. Henikoff, Nat. Struct. Mol. Biol. **20**, 259 (2013).

[19] A. Klosin, K. Reis, C. Hidalgo-Carcedo, E. Casas, T. Vavouri, and B. Lehner, Sci. Adv. **3** (2017), 10.1126/sciadv.1701143.

[20] T. K. Barth and A. Imhof, Trends Biochem. Sci. **35**, 618 (2010).

[21] T. B. Kheir and A. H. Lund, Essays Biochem. **48**, 107 (2010).

[22] C. Alabert, T. K. Barth, N. Reverón-Gómez, S. Sidoli, A. Schmidt, O. Jensen, A. Imhof, and A. Groth, Genes Dev. **29**, 585 (2015).

[23] P. J. Skene and S. Henikoff, Development **140**, 2513 (2013).

[24] A. N. D. Scharf, T. K. Barth, and A. Imhof, Nucleic Acids Res. **37**, 5032 (2009).

[25] C. Arnold, P. F. Stadler, and S. J. Prohaska, J. Theor. Biol. **336**, 61 (2013).

[26] I. B. Dodd, M. A. Micheelsen, K. Sneppen, and G. Thon, Cell **129**, 813 (2007).

[27] S. Berry, C. Dean, and M. Howard, Cell Syst. **4**, 445 (2017).

[28] T. Sexton, E. Yaffe, E. Kenigsberg, F. Bantignies, B. Leblanc, M. Hoichman, H. Parrinello, A. Tanay, and G. Cavalli, Cell **148**, 458 (2012).

[29] J. R. Dixon, S. Selvaraj, F. Yue, A. Kim, Y. Li, Y. Shen, M. Hu, J. S. Liu, and B. Ren, Nature **485**, 376 (2012).

[30] D. Jost, P. Carrivain, G. Cavalli, and C. Vaillant, Nucleic Acids Research **42**, 1 (2014).

[31] S. S. P. Rao, M. H. Huntley, N. C. Durand, E. K. Stamenova, I. D. Bochkov, J. T. Robinson, A. L. Sanborn, I. Machol, A. D. Omer, E. S. Lander, and E. L. Aiden, Cell **159**, 1665 (2014).

[32] J. R. Dixon, I. Jung, S. Selvaraj, Y. Shen, J. E. Antosiewicz-Bourget, A. Y. Lee, Z. Ye, A. Kim, N. Rajagopal, W. Xie, Y. Diao, J. Liang, H. Zhao, V. V. Lobanenkov, J. R. Ecker, J. A. Thomson, and B. Ren, Nature **518**, 331 (2015).

[33] M. A. Micheelsen, N. Mitarai, K. Sneppen, and I. B. Dodd, Phys. Biol. **7**, 026010 (2010).

[34] I. B. Dodd and K. Sneppen, J. Mol. Biol. **414**, 624 (2011).

[35] L. C. M. Anink-Groenen, T. R. Maarleveld, P. J. Verschure, and F. J. Bruggeman, Epigenetics chromatin **7**, 30 (2014).

[36] M. J. Obersriebnig, E. M. H. Pallesen, K. Sneppen, A. Trusina, and G. Thon, Nat. Commun. **7**, 11518 (2016).

[37] F. Erdel and E. C. Greene, Proc. Nat. Acad. Sci. USA **113**, E4180 (2016).

[38] P. B. Talbert and S. Henikoff, Nat. Rev. Genet. **7**, 793 (2006).

[39] C. Lanzuolo, V. Roure, J. Dekker, F. Bantignies, and V. Orlando, Nat. Cell Biol. **9**, 1167 (2007).

[40] J. M. Engreitz, A. Pandya-jones, P. Mcdonel, A. Shishkin, K. Sirokman, C. Surka, S. Kadri, J. Xing, A. Goren, E. S. Lander, K. Plath, and M. Guttman, Science **341**, 1 (2013).

[41] S. F. Pinter, R. I. Sadreyev, E. Yildirim, Y. Jeon, T. K. Ohsumi, M. Borowsky, and J. T. Lee, Genome Res. **22**, 1864 (2012).

[42] T. Schauer, Y. Ghavi-Helm, T. Sexton, C. Albig, C. Regnard, G. Cavalli, E. E. Furlong, and P. B. Becker, EMBO reports (2017).

[43] W. Deng, J. W. Rupon, I. Krivega, L. Breda, I. Motta, K. S. Jahn, A. Reik, P. D. Gregory, S. Rivella, A. Dean, and G. A. Blobel, Cell **158**, 849 (2014).

[44] D. Michieletto, E. Orlandini, and D. Marenduzzo, Phys. Rev. X **6**, 041047 (2016).

[45] N. A. Hathaway, O. Bell, C. Hodges, E. L. Miller, D. S. Neel, and G. R. Crabtree, Cell **149**, 1447 (2012).

[46] S. Hauri, F. Comoglio, M. Seimiya, M. Gerstung, T. Glatter, K. Hansen, R. Aebersold, R. Paro, M. Gstaiger, and C. Beisel, Cell Rep. **17**, 583 (2016).

[47] A. Collinson, A. J. Collier, N. P. Morgan, A. R. Sienerth, T. Chandra, S. Andrews, and P. J. Rugg-Gunn, Cell Rep. **17**, 2700 (2016).

[48] S. S. Teves, L. An, A. S. Hansen, L. Xie, X. Darzacq, and R. Tjian, Elife **5**, 1 (2016).

[49] J. A. Kassis and J. L. Brown, Advances in genetics **81**, 83 (2013).

[50] B. Schuettengruber, N. Oded Elkayam, T. Sexton, M. Entrevan, S. Stern, A. Thomas, E. Yaffe, H. Parrinello, A. Tanay, and G. Cavalli, Cell Rep. **9**, 219 (2014).

[51] F. Laprell, K. Finkl, and J. Müller, Science **8266**, eaai8266 (2017).

[52] N. E. Follmer, A. H. Wani, and N. J. Francis, PLoS Genet. **8** (2012).

[53] S. Kadauke, M. I. Udugama, J. M. Pawlicki, J. C. Achtman, D. P. Jain, Y. Cheng, R. C. Hardison, and G. A. Blobel, Cell **150**, 725 (2012).

[54] S. Kadauke and G. A. Blobel, Epigenetics chromatin **6**, 6 (2013).

[55] A. Grob, C. Colleran, and B. McStay, Genes Dev. **28**, 220 (2014).

[56] N. Festuccia, A. Dubois, S. Vandormael-Pournin, E. G. Tejeda, A. Mouren, S. Bessonnard, F. Mueller, C. Proux, M. Cohen-Tannoudji, and P. Navarro, Nat. Cell Biol. **18**, 1139 (2016).

[57] C. Deluz, E. T. Friman, D. Strebinger, A. Benke, M. Raccaud, A. Callegari, M. Leleu, S. Manley, and D. M. Suter, Genes Dev. **30**, 2538 (2016).

[58] P. V. Kharchenko, A. A. Alekseyenko, Y. B. Schwartz, A. Minoda, N. C. Riddle, J. Ernst, P. J. Sabo, E. Larschan, A. A. Gorchakov, T. Gu, D. Linder-Basso, A. Plachetka, G. Shanower, M. Y. Tolstorukov, L. J. Luquette, R. Xi, Y. L. Jung, R. W. Park, E. P. Bishop, T. K. Canfield, R. Sandstrom, R. E. Thurman, D. M. MacAlpine, J. A. Stamatoyannopoulos, M. Kellis, S. C. R. Elgin, M. I. Kuroda, V. Pirrotta, G. H. Karpen, and P. J. Park, Nature **471**, 480 (2011).

[59] N. Gilbert and W. A. Bickmore, Biochem. Soc. Symp. **73**, 59 (2006).

[60] A. Rosa and R. Everaers, PLoS Comp. Biol. **4**, 1 (2008).

[61] G. Fudenberg, M. Imakaev, C. Lu, A. Goloborodko, N. Abdennur, and L. A. Mirny, Cell Rep. **15**, 2038 (2016).

[62] L. A. Mirny, Chromosom. Res. **19**, 37 (2011).

[63] C. A. Brackley, J. Johnson, S. Kelly, P. R. Cook, and D. Marenduzzo, Nucleic Acids Res. **44**, 3503 (2016).

[64] C. A. Brackley, D. Michieletto, F. Mouvet, J. Johnson, S. Kelly, P. R. Cook, and D. Marenduzzo, Nucleus **7**, 453 (2016).

[65] C. A. Brackley, S. Taylor, A. Papantonis, P. R. Cook, and D. Marenduzzo, Proc. Natl. Acad. Sci. USA **110**, E3605 (2013).

[66] T. M. Cheng, S. Heeger, R. A. Chaleil, N. Matthews, A. Stewart, J. Wright, C. Lim, P. A. Bates, and F. Uhlmann, Elife **4**, 1 (2015).

[67] A. L. Sanborn, S. S. P. Rao, S.-C. Huang, N. C. Durand, M. H. Huntley, A. I. Jewett, I. D. Bochkov, D. Chinnappan, A. Cutkosky, J. Li, K. P. Geeting, A. Gnirke, A. Melnikov, D. McKenna, E. K. Stamenova, E. S. Lander, and E. L. Aiden, Proc. Natl. Acad. Sci. USA **112**, 201518552 (2015).

[68] A. Rosa, N. B. Becker, and R. Everaers, Biophys. J. **98**, 2410 (2010).

[69] M. Di Pierro, B. Zhang, E. L. Aiden, P. G. Wolynes, and J. N. Onuchic, Proc. Natl. Acad. Sci. USA **113**, 201613607 (2016).

[70] M. Barbieri, M. Chotalia, J. Fraser, L.-M. Lavitas, J. Dostie, A. Pombo, and M. Nicodemi, Proc. Natl. Acad. Sci. USA **109**, 16173 (2012).

[71] N. Gilbert, S. Gilchrist, and W. A. Bickmore, Int. Rev. Cytol. **242**, 283 (2004).

[72] R.-S. Nozawa, L. Boteva, D. C. Soares, C. Naughton, A. R. Dun, B. Ramsahoye, P. C. Bruton, R. S. Saleeb, M. Arnedo, B. Hill, R. Duncan, S. K. Maciver, and N. Gilbert, Cell (2017).

[73] D. Michieletto, E. Orlandini, and D. Marenduzzo, arXiv:1705.03226 , 1 (2017).

[74] G. Schotta, A. Ebert, V. Krauss, A. Fischer, J. Hoffmann, S. Rea, T. Jenuwein, R. Dorn, and G. Reuter, EMBO J. **21**, 1121 (2002).

[75] K. D. Sarge and O. K. Park-Sarge, Trends Biochem. Sci. **30**, 605 (2005).

[76] T. Cheutin and G. Cavalli, PLoS Genet. **8** (2012).

[77] E. Lieberman-Aiden, N. L. van Berkum, L. Williams, M. Imakaev, T. Ragoczy, A. Telling, I. Amit, B. R. Lajoie, P. J. Sabo, M. O. Dorschner, R. Sandstrom, B. Bernstein, M. A. Bender, M. Groudine, A. Gnirke, J. Stamatoyannopoulos, L. A. Mirny, E. S. Lander, and J. Dekker, Science **326**, 289 (2009).

[78] S. Berry, M. Hartley, T. S. G. Olsson, C. Dean, and M. Howard, Elife **4**, 1 (2015).

[79] R. T. Coleman and G. Struhl, Science **8236**, 10.1126/science.aai8236 (2017).

[80] To determine these probability, a bookmarked bead is counted as bearing the H3K27me3 mark when it is near beads with polycomb marks, or within large stretches of bookmarked beads.

[81] C. A. Brackley, B. Liebchen, D. Michieletto, F. Mouvet, P. R. Cook, and D. Marenduzzo, Biophys J. **112**, 1085 (2017).

[82] S. De, A. Mitra, Y. Cheng, K. Pfeifer, and J. A. Kassis, PLoS Genet. **12**, 1 (2016).

[83] I. Kirmes, A. Szczurek, K. Prakash, I. Charapitsa, C. Heiser, M. Musheev, F. Schock, K. Fornalczyk, D. Ma, U. Birk, C. Cremer, and G. Reid, Genome Biol. **16**, 246 (2015).

[84] J. M. Caravaca, G. Donahue, J. S. Becker, X. He, C. Vinson, and K. S. Zaret, Genes Dev. **27**, 251 (2013).